ALKU Journal of Science 2024, Sayı 6(1): 66-79
e-ISSN: 2667-7814

Original Article

Robust Direct Power Flow Control of Voltage Source Converters

Akin Uslu[1*], Emrah Irmak[1]
[1]*Department of Electrical and Electronics Engineering, Alanya Alaaddin Keykubat University, Antalya, Turkey*
**akin.uslu@alanya.edu.tr*

Abstract

In this study, a disturbance observer-based power control system is developed for voltage source converters (VSC) to achieve smooth power delivery to the grid. Firstly, modelling of grid connected converter which is used for power delivery in terms of frequency and current dynamics is executed under consideration of modelling errors and uncertainties. This disturbance effects are mainly consist of frequency and amplitude variations, output impedance aging, large dc-link voltage ripple. A nonlinear observer is integrated into the controller in order to reject model uncertainty and disturbances of the system. Due to the objective of the proposed controller is power regulation, there is no need voltage and current compensator. Simulation comparisons are carried out to verify the robustness of the proposed controller. Also the effectiveness of the proposed approach is tested under different grid scenarios (e.g., weak grid, dc-link variation, frequency deviation)

Keywords: Direct power control (DPC), Grid disturbance, Model errors, Parametric uncertainty

Gerilim Kaynaklı Dönüştürücülerin Gürbüz Doğrudan Güç Akış Kontrolü

Özet

Bu çalışmada, gerilim kaynaklı dönüştürücüler için bozucu etki gözlemleyicisi tabanlı bir bir güç kontrol sistemi geliştirilmiştir. İlk olarak, güç dağıtımı için kullanılan şebeke bağlantılı dönüştürücülerin frekan ve akım dinamikleri modelleme hatası ve belirsizlikleri göz önüne alınılanarak modellemesi gerçekleştirilmiştir. Bu bozucu etkiler çoğunlukla frekans ve genlik dalgalanmaları, çıkış empedansındaki eskime ve dc hat gerilim dalgalanmalarından oluşur. Sistemin model belirsizlikleri ve bozucu etkilerini engellemek amacıyla bir doğrusal olmayan gözlemleyici denetleyiciye entegre edilmiştir. Önerilen denetleyicinin amacı güç dengesini sağlamak olduğu için gerilim ve akım denetleyicileri ihtiyac duyulmaz. Önerilen denetleyicinin gürbüzlüğü simulasyon çalışmaları ile doğrulanmıştır. Ayrıca, önerilen denetleyicinin verilimliği Çeşitli şebeke senaryoları (zayıf şebeke, dc hat dalgalanmaları, frekans değişimi) altında test edilmiştir.

Anahtar Kelimeler: Doğrudan güç kontrolü (DGC), Şebeke bozucu etkisi, Model hataları, parametrik belirsizlikler

Geliş/Received: 4 Aralık/December 2023
Kabul Ediliş/Accepted: 7 Aralık/December 2023

1. INTRODUCTION

Although DC/ac pulse width modulated (PWM) voltage source converters (VSC) are widely used in industrial applications, they face some difficulties during grid integration. Uninterruptible power supplies require high power factor, the low current harmonics for public utility, and motor drives for railway traction need bidirectional energy flow, and steady dc input voltage [1]-[5]. Besides, the renewable energy connected VSC, wind turbine system and photovoltaics are faced fluctuating dc-link voltage in changing atmospheric conditions like wind or sunlight irradiation; the uncertainties of grid power parameters (frequency, amplitude,phase) effect the stability of the operation of VSC.

Several nonlinear control approaches have been proposed for VSC to obtain satisfactory transient performance and against to the unmodelling dynamics, such as model predictive control (MPC) [6,7], lyapunov based control [8], proportional reononant based control [9], proportional integral (PI) control [10] and direct power control (DPC) [11,12].

Among these techniques, DPC can be considered as a suitable candidate for three phase VSC, due to it's the instantaneous power theory basis [13]. The DPC aproach directly uses instantaneous active and reactive power components as control states instead of current and voltage variables commonly used in the voltage-oriented control (VOC) [14]. Two key factors play important roles in the performance of DPC approach: one is obtaining precise values of the instantaneous active and reactive power; the other is the accurate field orientation for grid voltage or virtual flux vector position [15,16]. Compared with the vector current control, the DPC scheme has fast dynamic power regulation response in some extreme conditions. To improve performance of the DPC, advanced strategies have been proposed such as model predictive DPC (MP-DPC) [17], fuzzy logic based DPC [18] and deadbeat DPC [19].

However, some drawbacks of DPC scheme in grid voltage parametric variations. One of them is the frequency dynamics are not modelled in the DPC, which makes it difficult to compensate the power angle between the VSC and the grid [20]. Another limitation is phase locked loop (PLL) that deteriorates the stability and the control response of VSC in weak grid conditions [21]. The the dc-link voltage variation can affect the stability of the VSC in the DPC [22] as well. The droop control for power flow with two paralled operated VSC have been videly used. It still has limitations to deal with parametric variations of grid voltage and requires additional control loops for current and voltage regulator [23].

In this paper, a composit power control strategy based on the nonlinear disturbance observer (NDO) aproach is constructed for VSC to transmit active and reactive power to the utility. The NDO is an complementary key tool for base controller that can observe and estimate the uncertainties independently of the controller [24],[25]. In recent years, the NDO-based methodology demonstrates its robustness performances in several industrial applications, such as power electronics [26], control of PMSM [27], and the variable-speed generators [28].

In this study, first step consists of power-based modelling of VSC system including both frequncy and voltage dynamics. The Second step is NDO which is integrated into the control law design to achive robust regulation for active and reactive power against to unmodelling dynamics such asimpedance variation and power factor angle, coupling effects due to grid frequency. Also, proposed scheme takes into account some dynamic distubances such as DC-link ripple and grid voltage variations.

Compact structure of the proposed approach simplifies the digital implemetation of the controller. Because the controlled states are active and reactive powers, there is no need to use voltage or current regulation. Proposed controller scheme provides seperated structure between desired tracking error dynamics and disturbance rejection. The effectiveness of the proposed approach is investigated by theoretical analysis and verified through simulation studies with the help of simulations in Matlab.

2. SYSTEM STRUCTURE AND CONTROL DESIGN

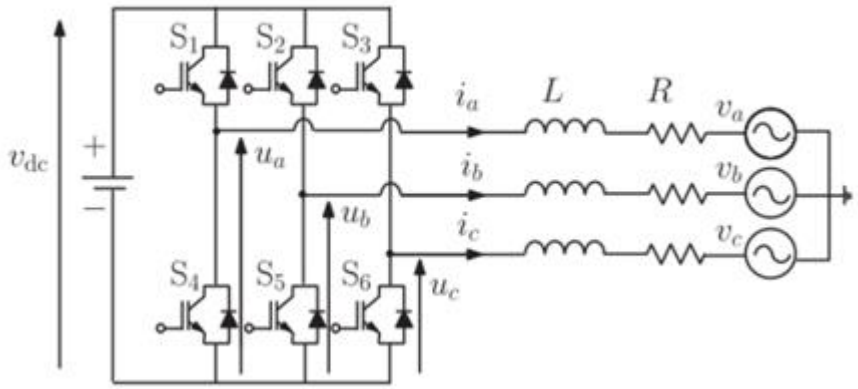

Figure 1. Three phase grid connected voltage source converter

Figure 1 shows schematic of the electrical connection of the three-phase two-level grid-connected voltage source converter (VSC). DC input voltage is tied to the converter via C capacitor which keeps the DC –link voltage constant. L and R are the equivalent inductor and resistance of the grid filter, respectively.

The dynamic model of the grid filter current in the d–q coordinates can be derived with the help Kirchhoff voltage law as follows:

$$\begin{cases} L\dfrac{di_d}{dt} = u_{cd} - Ri_d + \omega Li_q - u_{gd} \\ L\dfrac{di_d}{dt} = u_{cq} - Ri_q - \omega Li_q - u_{gq} \end{cases} \tag{1}$$

where $u_{cd}$and u_{cq} are the control functions, u_{gd} and $u_{gq}$are the grid voltages, i_d and i_q are the converter filter currents, and ω represents the nominal angular frequency.

According to basics of of the instantaneous power theory, the active power P and reactive power Q are given as as follows:

$$\begin{cases} P = \dfrac{1}{2}(u_{gd}i_d + u_{gq}i_q) \\ Q = \dfrac{1}{2}(u_{gq}i_d - u_{gd}i_q) \end{cases} \tag{2}$$

Then, the differential values of active and reactive powers are derived as:

$$\begin{aligned} \frac{dP}{dt} &= \left[\frac{du_{gd}}{dt}i_d + \frac{di_d}{dt}u_{gd} + \frac{du_{gq}}{dt}i_q + \frac{di_q}{dt}u_{gq}\right] \\ \frac{dQ}{dt} &= \left[\frac{du_{gq}}{dt}i_d + \frac{di_d}{dt}u_{gq} - \frac{du_{gd}}{dt}i_q - \frac{di_q}{dt}u_{gd}\right] \end{aligned} \tag{3}$$

Assuming components of grid voltage in d–q rotating frame are constant, dynamics of (3) active and reactive powers can be reformulated as:

$$\begin{cases} \dot{P} = -\frac{R}{L}P - \omega Q - \frac{u_g^2}{2L} + \frac{u_{cd}u_g}{2L} \\ \dot{Q} = -\frac{R}{L}Q + \omega P - \frac{u_{cq}u_g}{2L} \end{cases} \quad (4)$$

(4) Can be considered as two part, which are dynamic and steady state component as follows:

$$\begin{cases} \dot{P} = \frac{u_{cd}u_g}{2L} + f_d \\ \dot{Q} = -\frac{u_{cq}u_g}{2L} + f_q \end{cases} \quad (5)$$

The dynamic part of the equation (5) can be compensated with controller, whereas steady state components additionally include lumped uncertain terms d_d and d_q caused by impedance variations from nominal values and coupling effects due to frequency changing. Lumped uncertainties are small and bounded which are given as:

$$\begin{cases} f_d = -\frac{R}{L}P - \omega Q - \frac{u_g^2}{2L} \\ f_q = -\frac{R}{L}Q + \omega P \end{cases} \quad (6)$$

With the approximation of the uncertain terms given in (6) and the dynamics of power (3) are converted to linear dynamics in (5) with the uncertain terms. This will simplify the controller design and also observer to estimate the uncertain terms for (5), which will be detailed in next section.

2.1 Controller Design

The control objective is to construct a control law that forces the reactive power Q and active power P tracking error which is defined in (7), converge to zero as t → ∞

$$e_q = Q_{ref} - Q \quad e_p = P_{ref} - P, \quad (7)$$

Where, $P_{ref}$and Q_{ref} represents active and reactive power reference, respectively. Assuming all the parameters of the VSC system are nominal value and disturbance parameters $f_d$and $f_q$are knowm. $P_{ref}$is obtained through the outer voltage control loop and Q_{ref} is generally set as 0. Here, a simple closed loop error equation is governed by,

$$\dot{e}_q = -K_q e_q, \quad \dot{e}_p = -K_P e_p \quad (8)$$

Where $K_P > 0$ and K_q>0 are the positive real feedback gains to ensure the asymptotic stability of (8). Putting together (5) and (8) gives

$$\dot{P}_{ref} - \frac{u_{cd}u_g}{2L} - f_d = -K_P e_p \quad (9)$$

$$\dot{Q}_{ref} + \frac{u_{cq}u_g}{2L} - f_q = -K_q e_q \quad (10)$$

With the assumption that grid voltage u_g is measurable and disturbance $f_d$and f_d are available, the control law for the the active and reactive powers can be derived as:

$$u_{cd} = \frac{2L}{u_g}\left[\dot{P}_{ref} - f_d + K_P e_p\right] \tag{11}$$

$$u_{cq} = -\frac{2L}{u_g}\left[\dot{Q}_{ref} - f_q + K_P e_q\right] \tag{12}$$

Specifically, the desired transient performance determines the control gain K_p and K_q . From a practical perspective, it is not possible to sense f_d and f_q disturbance; the only available signal is grid voltage u_g. By implementing control law with the estimation of disturbance $\hat{f}_d$ and $\hat{f}_q$ instead of f_d and f_q solves this issue, yielding;

$$u_{cd} = \frac{2L}{u_g}\left[\dot{P}_{ref} - \hat{f}_d + K_P e_p\right] \tag{13}$$

$$u_{cq} = \frac{2L}{u_g}\left[\dot{P}_{ref} - \hat{f}_q + K_Q e_p\right] \tag{14}$$

2.2 Observer Design

With the assumption that disturbance is boundedand its bound is constrained with $\dot{f}_d = 0$, $\dot{f}_q = 0$ and considering active and reactive power are measurable, an observer can be derived as fallows [25]:

$$\dot{\hat{f}}_d = -l_d\hat{f}_d + l_d(\dot{P} - \frac{u_{cd}u_g}{2L}) \tag{15}$$

$$\dot{\hat{f}}_q = -l_q\hat{f}_q + l_q(\dot{P} - \frac{u_{cd}u_g}{2L}) \tag{16}$$

Where l_d and l_q are observer gains. Following, (5) and (11) estimation error of disturbance $\tilde{f}_d$=$\hat{f}_d$−f_d and $\tilde{f}_q$=$\hat{f}_q$−f_q are governed by

$$\dot{\tilde{f}}_d = -l_d\tilde{f}_d \tag{17}$$

$$\dot{\tilde{f}}_q = -l_q\tilde{f}_d \tag{18}$$

It is obvious that observer error dynamics in (17,18) can be made stable by selecting the gain parameters l_d>0 and l_q>0. It is clear the observer estimation error converges to zero with

$$lim_{t\to\infty} f_d = 0 \tag{19}$$

$$lim_{t\to\infty} f_q = 0 \tag{20}$$

When choosing observer gain for practical application, there are some concern to take into attention. According to (11), fast estimation response can be obtained with high observer gain [l_d, l_q]. In addition, it causes large measurement noises. Thus, a trade off between a fast estimation response and measurement noises reduction is needed to prevent large the state fluctuations. The other concern about the related DO is that in digital implementation the derivative of the state that can not be processed because it is not available. Such a drawback can be circumvented by reformulating the proposed DO as follows:

$$\begin{cases} \dot{z}_d = -l_d z_d - l_d[\frac{u_{cd}u_g}{2L} + l_d z_d] \\ \dot{z}_q = -l_q z_q - l_q[\frac{u_{cq}u_g}{2L} + l_q z_q] \end{cases} \tag{21}$$

where z is an auxiliary variable which is used to get rid of time derivation of the state. Selecting z(0) = −p(x(0)), the estimation can be preserved in the condition that there is no disturbances.

3. STABILITY AND STEADY STATE PERFORMANCE ANALYSIS

3.1 Stability Analysis

Considering the VSC supplying power to the grid with the dynamic equation (5), and the NDO-based direct power control function (11) and (12), if the disturbance terms are bounded, then the closed-loop system stablity is guaranteed in the sense of boundedness,for all $t \geq 0$.
proof. Considering the Lyapunov stability function:

$$V(t) = \frac{1}{2}({e_p}^2 + {e_q}^2) \tag{22}$$

Deviration of $V(t)$ along (8) gives:

$$\begin{aligned} \dot{V}(t) &= \dot{e}_p e_p + \dot{e}_q e_q \\ &= e_p\left(\dot{P}_{ref} - \frac{u_{cd}u_g}{2L} - f_d\right) + e_q(\dot{Q}_{ref} + \frac{u_{cq}u_g}{2L} - f_q) \end{aligned} \tag{23}$$

With the NDO-based DPC laws (13) and (14), and along with (21),

$$\begin{aligned} \dot{V}(t) &= e_p\left(-K_P e_p + \hat{f}_d - f_d\right) + e_q\left(-K_Q e_q + \hat{f}_q - f_q\right) \\ &= -K_P {e_p}^2 - K_Q {e_q}^2 - e_p\tilde{f}_d - e_q\tilde{f}_q \end{aligned} \tag{24}$$

if the lumped uncertainty terms f_d and f_q are bounded and observer parameter l_d and l_q are large enough, then estimation errors $\tilde{f}_d$ and $\tilde{f}_q$ can be considered as bounded. With the help of Young's inequality, (23) can be reformulated as,

$$\dot{V}(t) \leq -K_P {e_p}^2 - K_Q {e_q}^2 + \frac{1}{2}\left({e_p}^2 + {e_q}^2\right) + \frac{1}{2}({\tilde{f}_d}^2 + {\tilde{f}_q}^2) \tag{25}$$

$$\dot{V}(t) = -\left(K_P - \frac{1}{2}\right){e_p}^2 - \left(K_Q - \frac{1}{2}\right){e_Q}^2 + \frac{1}{2}({\tilde{f}_d}^2 + {\tilde{f}_q}^2) \tag{26}$$

$$\dot{V}(t) \leq -\sigma_1 V(t) + \sigma_2 \tag{27}$$

Where, $\sigma_1 = min\{2K_P - 1, 2K_Q - 1\} > 0$, $\sigma_2 > 0$ is top bound for $V(t)$. Then evaluating (25)-(27) gives:

$$V(t) \leq V(0)e^{-\sigma_1 t} + \frac{\sigma_2}{\sigma_1}(1 - e^{-\sigma_1 t}) \tag{28}$$

The bounds of e_p and e_q can be tuned through the control feedback gains K_p , K_q. Estimation accuracy of disturbance terms $\hat{f}_d$ and $\hat{f}_q$ depend on observer gains l_d and l_q which make error tracking convergent to zero.

3.2 Performance Analysis

When the observed terms $\hat{f}_d$ and $\hat{f}_q$ are substituted in (11) and (12) and to replace f_d and f_q, control error dynamics in (8) can be rewritten as:

$$\dot{e}_p = -K_P e_p - \tilde{f}_d \tag{29}$$

$$\dot{e}_q = -K_Q e_Q - \tilde{f}_q \tag{30}$$

Substituting (17) and (18) into (29) and (30), control error dynamics in frequency domain can be described as,

$$se_p(s) = -K_P e_p(s) - f_d(s)\left[\frac{s}{s+l_d}\right] \tag{31}$$

$$se_q(s) = -K_Q e_q(s) - f_q(s)\left[\frac{s}{s+l_q}\right] \tag{32}$$

Where $e_p(s)$, $e_q(s)$, $f_d(s)$ and $f_q(s)$ are laplace transform of e_p, e_q, f_d and f_q. Then,

$$e_p(s) = -f_d(s)\left[\frac{s}{(s+K_P)(s+l_d)}\right] \tag{33}$$

$$e_q(s) = -f_q(s)\left[\frac{s}{(s+K_Q)(s+l_q)}\right] \tag{34}$$

It is assumed that disturbance values $f_d(s)$ and $f_q(s)$ are bounded.

$$\lim_{s\to 0} s.f_d(s) < 0 \tag{35}$$

$$\lim_{s\to 0} s.f_q(s) < 0 \tag{36}$$

by applying the final value theorem to (33) and (34), there are;

$$\lim_{t\to 0} e_p(s) = -\lim_{s\to 0} f_d(s)\left[\frac{s}{(s+K_P)(s+l_d)}\right] = 0 \tag{37}$$

$$\lim_{t\to 0} e_q(s) = -\lim_{s\to 0} f_q(s)\left[\frac{s}{(s+K_Q)(s+l_q)}\right] = 0 \tag{38}$$

From (37), (38) it can be seen that the average values of tracking errors for active and reactive power converge to zero as time goes infinity. This means stable power delivery to the grid is obtained.

4. SIMULATION STUDIES

Some simulation studies were conducted to observe the performance of the proposed controller. The block diagram for simulate the proposed controller is represented in Fig. 2. The experimental parameters of the grid-connected system can be listed as: Filter inductor is L = 8 mH, dc-link voltage V_{dc} 300 V, grid frequency 50 Hz, and maximum value of grid voltage is 110 Vrms, filter resistance R=1 Ω. The sampling frequency for the controller is tuned to 10 kHz. The three-phase voltage references are generated by the proposed controller scheme must be converted into modulating signals da , db , and dc for PWM carrier wave. PWM modulation was conducted for modulating signals to produce the gating signal for the three-phase inverter. The switching frequency for the PWM is selected as 10 khz. Simulations were carried out on Matlab.

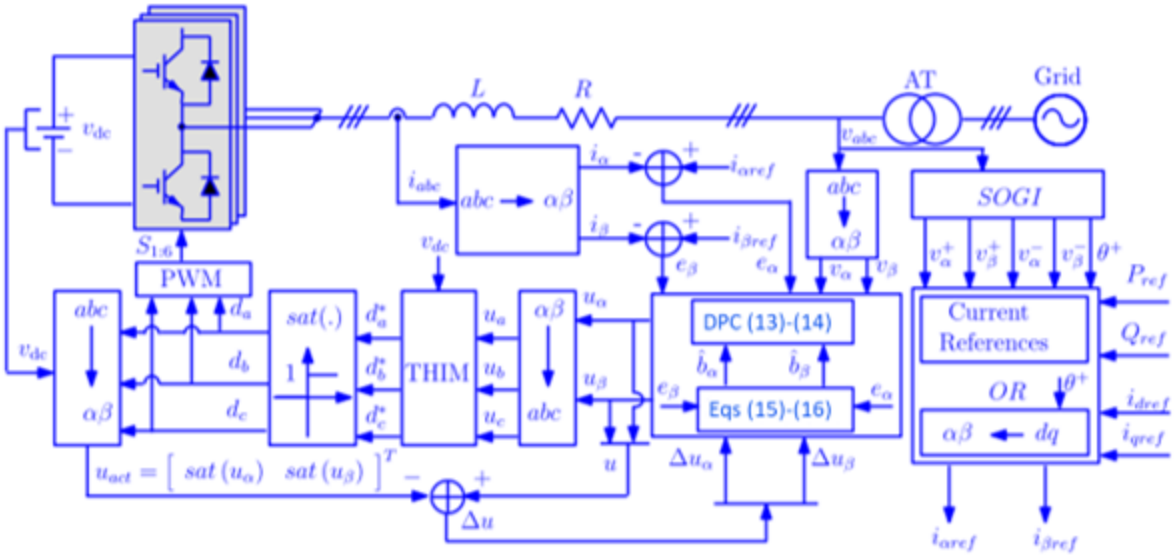

Figure 2. Proposed control system for VSC

To obtain the desired tracking error dynamics, parameter constant for feedback gain are selected as K_p = K_q= 10. Basically, the control gain K_p and K_q determines the closed loop response in the dq reference frame. By making use of (29)–(30), it is clear that the time constant of the closed-loop system, 1/K_p and 1/ K_p are on the order of 1 ms. The observer feedback parameters l_d and l_q is calculated according to (17),(18). In order to obtain a better estimation of disturbance terms f_p and f_p , the bandwidth of the observer filter should be bigger than time constant of desired step response 1/K_p, and 1/ K_p. Under bandwith limitation, the observer parameters are chosen as l_d =25 and l_q =25 To estimate the components of the grid voltage (e.g., phase and amplitude), second-order generalized integrator (SOGI) phase-locked-loop is integrated in the control loop.

4.1 Dynamic Reponse of Proposed Control

Fig. 3 shows the grid currents and the active and reactive powers of inverter when a reference power step is changed suddenly. The active power is increased from 0.75 kW to 1.5 kW, whereas the reactive power reference steps is set from 0 to 0.5 kVAr and from 0.5 kVAr to 0. As it can be seen, the active and reactive powers have a fast transient response. Also, a small fluctuation is observed.

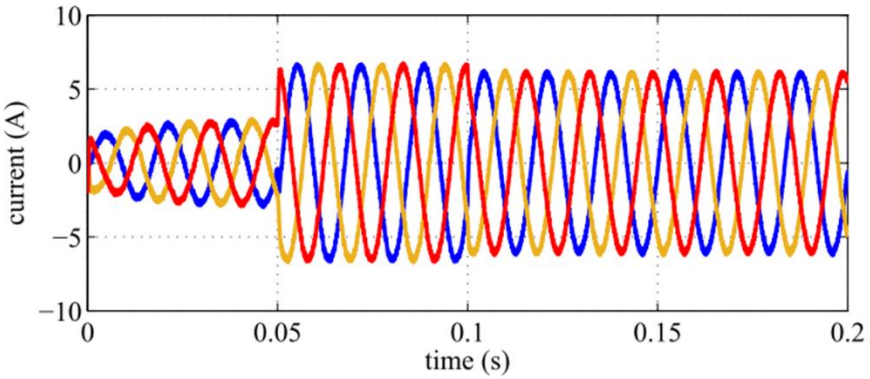

(a)

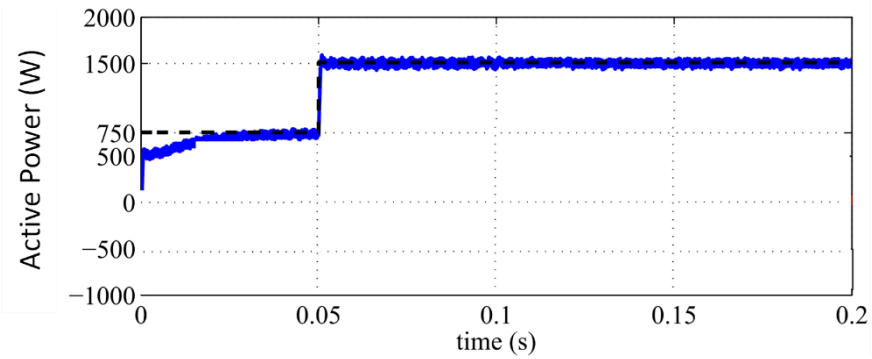

(b)

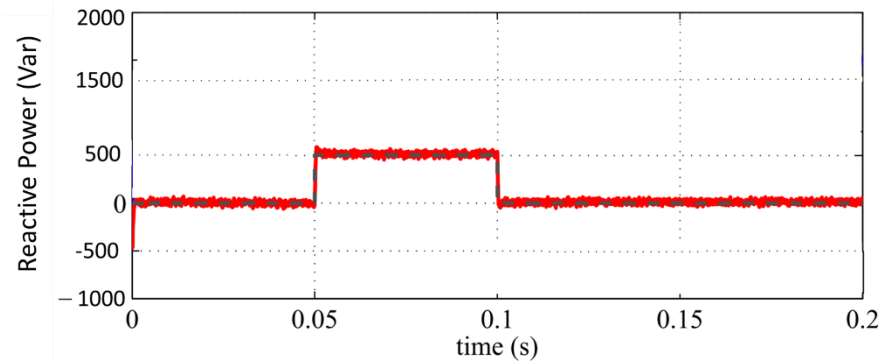

(c)

Figure 3. Step change of power
(a) three phase currents (b) active power (c) reactive power

4.2 Performance Analysis with Impedance Uncertainties and Input Voltage Disturbances

In this case of simulation, input voltage magnitude of inverter is deliberately changed by keeping the voltage and frequency of grid in default value. The simulation takes 30 sn. At time t = 5 s. reference value of active power is set P_{ref}= 100 W, and reactive power is Q_{ref}= −50 Var. 10 sn later, active power is decreased to 50 W, and reactive power is increased to −25 Var. Finally input voltage is reduced from 300 to 250 V at t = 20 sn and returns to 300 V 5 sn later.

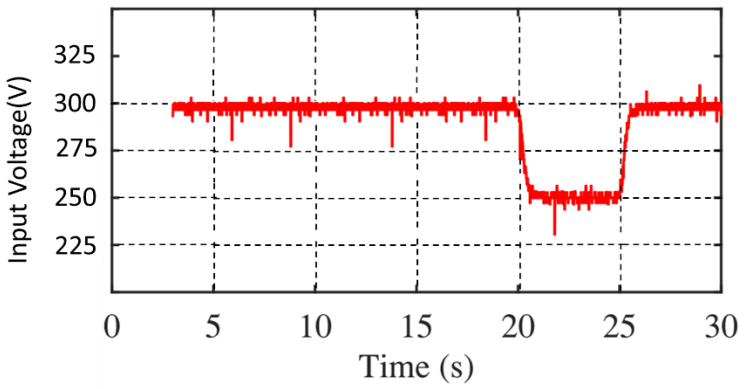

(a)

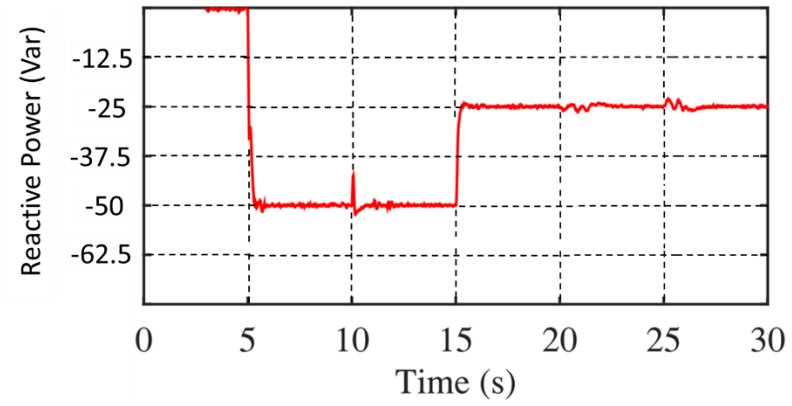

(b)

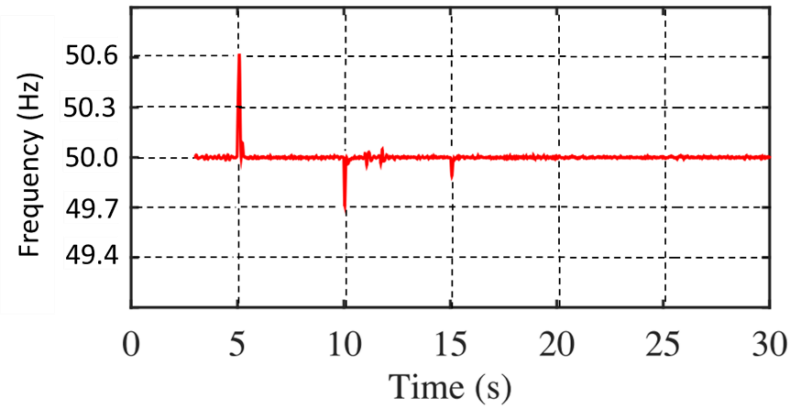

(c)

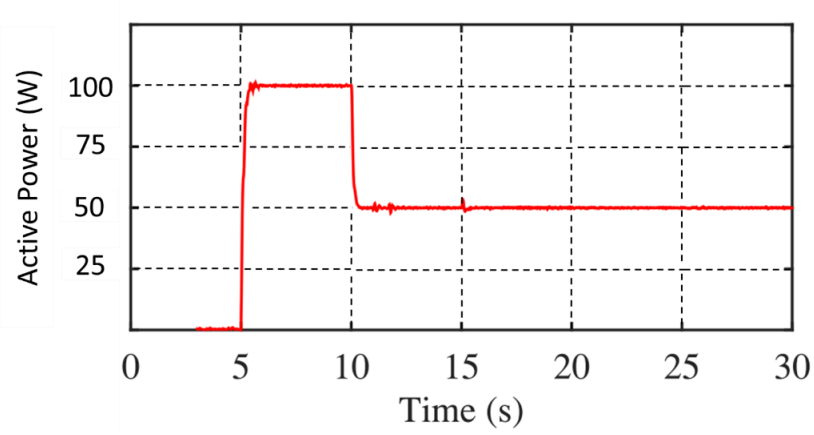

(d)

Figure 4. Dc-link input voltage variation
(a) input voltage (b) reactive power (c) frequency (d) active power

The esimulation result are shown in Fig. 4. After 5sn later, real power and reactive power are settle down at the reference values P = 100 W and Q = −50 Var respectively. Transient response takes 0.5 sn with a small overshoot. As shown in Fig. 4b, the variation real power causes a positive and negative frequency bounce ant time t = 5 s and t = 15s respectively. Then inverter frequency reaches its nominal value quickly.

4.3 Robustness Analysis of Proposed Control

Robustness of the proposed controller is studies with addition of virtual resistance which is shown in Fig. 5. Default references for active and reactive powers is not changed until t=5sn (P_{ref}, P_{ref})=(100W,-50Var). A virtual resistance is added at t=10sn and then returned to the nominal value to emulate uncertainty of output impedance. It is observed that reactive power has big bounce for about %25 of its nominal value at t=10sn and t=20 sn. Then, it converges to the set reference value within 0.5 sn. As shown in Fig. 5, resistance variation of the system causes small spikes on the real power and grid frequency.

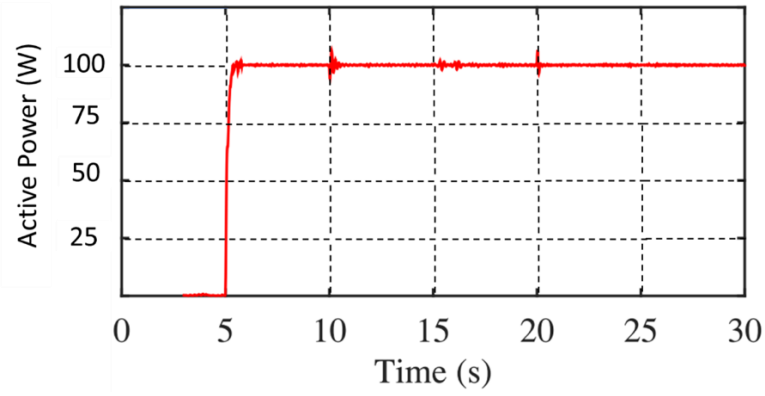

(a)

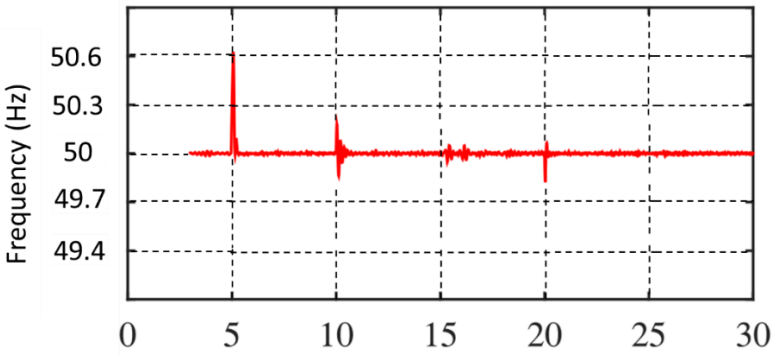

(b)

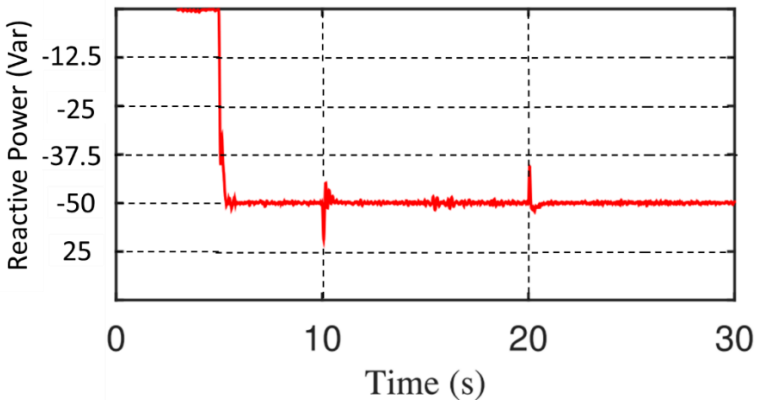

(c)

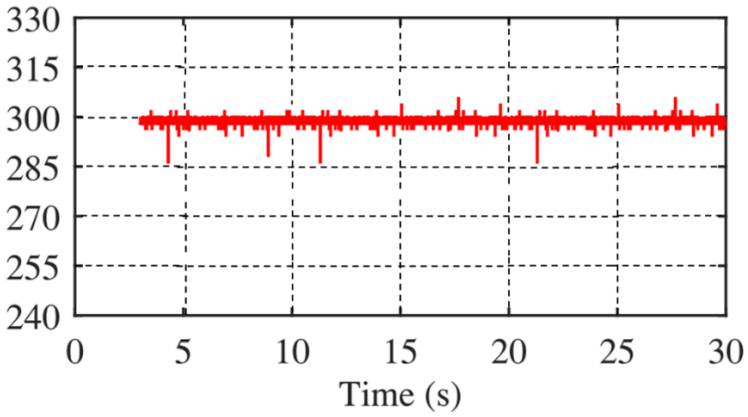

(d)

Figure 5. Grid impedance variation
(a) input voltage (b) reactive power (c) frequency (d) active power

the variation of grid impedance is observed wtih virtually added inductor in Fig 5. Robustness are almost same with the case of resistance variation. We can say that sytem resonponse to disturbance effect of resistance and inductor variation are similar.

5. CONCLUSION

In this study, a novel NDO strategy based on DPC scheme was built for voltage source converter to improve the disturbance rejection and robustness against the perturbations while achieving satisfactory dynamic performance. The detailed power model of the VSC is developed. Proposed method provides a unified control approach with the closed loop response and attenuation of disturbance which are considered as lumped disturbance. Control gains of NDO-DPC can be designed separately for the desired closed loop response and disturbance rejection. In addition, computational and PWM delays have been considered as lumped uncertainty while construction of proposed control system. Compared with the DPC-NDO and classical DPC, the proposed NDO-DPC has faster dynamic response and could reach the given references with zero tracking error under parametric variations. In order to select the control gains of the proposed NDO-DPC based on desired transient response specifications, an analytical parameter tuning method has been developed. Finally, the proposed control approach was verified by the comparative simulation and experimental results with Matlab.

REFERANSLAR

[1] Z. Zheng, Z. Gao, C. Gu, L. Xu, K. Wang, and Y. Li, “Stability and voltage balance control of a modular converter with multiwinding highfrequency transformer,” IEEE Trans. Power Electron., vol. 29, no. 8, pp. 4183–4194, Aug. 2014.

[2] M. Kabalo, D. Paire, B. Blunier, D. Bouquain, M. G. Simoes, and A. Miraoui, “Experimental evaluation of four-phase floating interleaved boost converter design and control for fule cell applications,” IET Power Electron., vol. 6, no. 2, pp. 215–216, Feb. 2013

[3] M. Prodanovic and T. C. Green, “Control and filter design of three-phase inverters for high power quality grid connection,” IEEE Trans. Power Electron., vol. 18, no. 1, pp. 373–380, Jan. 2003

[4] T. F. Zhao, G. Y. Wang, S. Bhattacharya, and A. Q. Huang, "Voltage and power balance control for a cascaded H-bridge converter-based solid-state transformer," IEEE Trans. Power Electron., vol. 28, no. 4, pp. 1523–1532, Apr. 2013.

[5] M. Rivera, V. Yaramasu, J. Rodriguez, and B. Wu, "Model predictive current control of two-level four-leg inverters—Part II: Experimental implementation and validation," IEEE Trans. Power Electron., vol. 28, no. 7, pp. 3469–3478, Jul. 2013.

[6] J. Hu, J. Zhu, and D. G. Dorrell, "Model predictive control of gridconnected inverters for PV systems with flexible power regulation and switching frequency reduction," IEEE Trans. Ind Appl., vol. 51, no. 1, pp. 587–594, Jan./Feb. 2015.

[7] V. Yaramasu, B. Wu, S. Alepuz, and S. Kouro, "Predictive control for low-voltage ride-through enhancement of three-level-boost and NPC converter- based PMSG wind turbine," IEEE Trans. Ind. Electron., vol. 61, no. 12, pp. 6832–6843, Dec. 2014

[8] Kato, T., Inoue, K., Ueda, M.: 'Lyapunov-based digital control of a grid-connected inverter with an LCL filter', IEEE J. Emerging Sel. Top. Power Electron., 2014, 2, (4), pp. 942–948.

[9] Castilla, M., Miret, J., Camacho, A., et al.: 'Reduction of current harmonic distortion in three-phase grid-connected photovoltaic inverters via resonant current control', IEEE Trans. Ind. Electron., 2013, 60, (4), pp. 1464–1472.

[10] M. Brenna, F. Foiadelli, and D. Zaninelli, "New stability analysis for tuning PI controller of power converters in railway application," IEEE Trans. Ind. Electron., vol. 58, no. 2, pp. 533–543, Feb. 2011.

[11] Y. Zhang and C. Qu, "Model predictive direct power control of PWM rectifiers under unbalanced network conditions," IEEE Trans. Ind. Electron., vol. 62, no. 7, pp. 4011–4022, Jul. 2015.

[12] P. Antoniewicz and M. P. Kazmierkowski, "Virtual-flux-based predictive direct power control of AC/DC converters with online inductance estimation," IEEE Trans. Ind. Electron., vol. 55, no. 12, pp. 4381–4390, Dec. 2008.

[13] H. Akagi, Y. Kanazawa, and A. Nabae, "Instantaneous reactive power compensators comprising switching devices without energy storage," IEEE Trans. Ind. Appl., vol. IA-20, no. 3, pp. 625–630, May/Jun. 1984.

[14] B. S. Chen and G. Joos, "Direct power control of active filters with averaged switching frequency regulation," IEEE Trans. Power Electron., vol. 23, no. 6, pp. 2729–2737, Jun. 2008.

[15] M. Malinowski, M. P. Kazmierkowski, S. Hansen, F. Blaabjerg, and G. D. Marquez, "Virtual-flux-based direct power control of three-phase PWM rectifiers," IEEE Trans. Ind. Appl., vol. 37, no. 4, pp. 1019–1027, Jul./Aug. 2001.

[16] R. Portillo, S. Vazquez, J. I. Leon, M. M. Prats, and L. G. Franquelo, "Model based adaptive direct power control for three-level NPC converters," IEEE Trans. Ind. Informat., vol. 9, no. 2, pp. 1148–1156, May 2013.

[17] M. Preindl, E. Schaltz, and P. Thogersen, "Switching frequency reduction using model predictive direct current control for high-power voltage source inverters," IEEE Trans. Ind. Electron., vol. 58, no. 7, pp. 2826– 2835, Jul. 2011.

[18] A. Bouafia, F. Krim, and J. P. Gaubert, “Fuzzy-logic-based switching state selection for direct power control of three-phase PWM rectifier,” IEEE Trans. Ind. Electron., vol. 56, no. 6, pp. 1984–1992, Jun. 2009.

[19] Bouafia, J. P. Gaubert, and F. Krim, “Predictive direct power control of three-phase pulsewidth modulation (PWM) rectifier using spacev ector modulation (SVM),” IEEE Trans. Power Electron., vol. 25, no. 1,pp. 228–236, Jan. 2010.

[20] P. Cortes, J. Rodriguez, P. Antoniewicz, and M. Kazmierkowski, “Direct power control of an AFE using predictive control,” IEEE Trans. Power Electron., vol. 23, no. 5, pp. 2516–2523, Sep. 2008.

[21] Q.-C. Zhong, P.-L.Nguyen, Z. Ma, andW. Sheng, “Self-synchronized synchronverters: Inverters without a dedicated synchronization unit,” IEEE Trans. Power Electron., vol. 29, no. 2, pp. 617–630, Feb. 2014.

[22] M. Monfared, M. Sanatkar, and S. Golestan, “Direct active and reactive power control of single-phase grid-tie converters,” IET Power Electron., vol. 5, no. 8, p. 1544, Sep. 2012.

[23] J. Kim, J. M. Guerrero, P. Rodriguez, R. Teodorescu, and K. Nam, “Mode adaptive droop control with virtual output impedances for an inverterbased flexible AC microgrid,” IEEE Trans. Power Electron., vol. 26,no. 3, pp. 689–701, Mar. 2011.

[24]] M. A. Hassan, T. Li, C. Duan, S. Chi, and E. P. Li, ‘‘Stabilization of DC-DC buck power converter feeding a mixed load using passivity-based control with nonlinear disturbance observer,’’ in Proc. IEEE Conf. Energy Internet Energy Syst. Integr. (EI2), Nov. 2017, pp. 1–6.

[25] M. A. Hassan, E.-P. Li, X. Li, T. Li, C. Duan, and S. Chi, ‘‘Adaptive passivity-based control of DC–DC buck power converter with constant power load in DC microgrid systems,’’ IEEE J. Emerg. Sel. Topics Power Electron., vol. 7, no. 3, pp. 2029–2040, Sep. 2019.

[26] L. Shengquan, L. Juan, T. Yongwei, S. Yanqiu, and C. Wei, ‘‘Modelbased model predictive control for a direct-driven permanent magnet synchronous generator with internal and external disturbances,’’ Trans. Inst. Meas. Control, vol. 42, no. 3, pp. 586–597, Feb. 2020.

[27] S. Li, M. Cao, J. Li, J. Cao, and Z. Lin, ‘‘Sensorless-based active disturbance rejection control for a wind energy conversion system with permanent magnet synchronous generator,’’ IEEE Access, vol. 7, pp. 122663–122674, 2019.

[28] R. Errouissi, M. Ouhrouche, W.-H. Chen, and A. M. Trzynadlowski, ‘‘Robust cascaded nonlinear predictive control of a permanent magnet synchronous motor with antiwindup compensator,’’ IEEE Trans. Ind. Electron., vol. 59, no. 8, pp. 3078–3088, Aug. 2012.